

Magnetic Rayleigh-Taylor Instability in Radiative Flows

Asiyeh Yaghoobi¹, Mohsen Shadmehri^{2*}

¹ *Department of Physics, Institute for Advanced Studies in Basic Sciences (IASBS), PO Box 11365-9161, Zanjan, Iran*

² *Department of Physics, Faculty of Sciences, Golestan University, Gorgan 49138-15739, Iran*

6 March 2018

ABSTRACT

We present a linear analysis of the radiative Rayleigh-Taylor (RT) instability in the presence of magnetic field for both optically thin and thick regimes. When the flow is optically thin, magnetic field not only stabilizes perturbations with short wavelengths, but also growth rate of the instability at long wavelengths is reduced compared to a nonmagnetized case. Then, we extend our analysis to the optically thick flows with a conserved total specific entropy and properties of the unstable perturbations are investigated in detail. Growth rate of the instability at short wavelengths is suppressed due to the presence of the magnetic field, however, growth rate is nearly constant at long wavelengths because of the radiation field. Since the radiative bubbles around massive protostars are subject to the RT instability, we also explore implications of our results in this context. In the nonmagnetized case, the growth time-scale of the instability for a typical bubble is found less than one thousand years which is very short compared to the typical star formation time-scale. Magnetic field with a reasonable strength significantly increases the growth time-scale to more than hundreds of thousands years. The instability, furthermore, is more efficient at large wavelengths, whereas in the non-magnetized case, growth rate at short wavelengths is more significant.

Key words: instabilities - MHD - H II regions - stars: formation

1 INTRODUCTION

Different types of instability have been proposed to understand some features of the astrophysical objects or formation of the structures in the astrophysical flows. Rayleigh-Taylor (RT) instability is an important mechanism which operates at the interface of two fluids with different densities while accelerating towards each other (Chandrasekhar 1961). The RT instability has found applications in various astrophysical systems, such as expansion of the supernova remnants (e.g., Ribeyre et al. 2004), bubbles in the intra-cluster medium (e.g., Pizzolato & Soker 2006; Jiang et al. 2013; Krumholz & Thompson 2012), prominences in the solar atmosphere (Terradas et al. 2012), and, interior of the red giants (e.g., Charbonnel & Lagarde 2010).

Linear growth rate of the RT instability and its non-linear evolution have been studied by many authors. For an incompressible flow, Chandrasekhar (1961) showed that the RT instability is suppressed, if the surface tension and the viscosity are considered. The effect of compressibility on the RT instability has been studied by Shivamoggi (2008) who showed that growth rate of the short-wavelength unstable perturbations decreases due to the compressibility. Since the RT instability may have an efficient role in some of

the magnetized astrophysical systems, the classical incompressible RT instability has also been extended to the magnetized case for a configuration with a uniform magnetic field parallel to the interface of the flows (Chandrasekhar 1961). The linear analysis shows that a tangential magnetic field reduces growth rate of the RT instability. Subsequent studies extended magnetized RT instability to the partially ionized systems where ions and neutrals as separate fluids can exchange momentum through direct collisions (e.g., Díaz et al. 2012; Shadmehri et al. 2013; Díaz et al. 2014). It is shown ion-neutral collision reduces the linear growth rate of the RT instability. Another important physical factor is the radiation field which may have a dynamically significant role in the RT instability. The radiation force, for instance, is significant at the boundary of a radiation-driven H II region (e.g., Jacquet & Krumholz 2011), or during massive star formation (e.g., Krumholz & Matzner 2009; Kumar 2013; Kuiper et al. 2012). Radiative RT instability has been studied by a few authors subject to simplifying assumptions (e.g., Mathews & Blumenthal 1977a; Krolik 1977). Detailed radiative RT instability in the linear regime for optically thin and thick systems has been formally analyzed by Jacquet & Krumholz (2011) (hereafter JK) for configurations with an isotropic radiation pressure. In the optically thin and isothermal regime, they showed that role of the radiation field is like an effective gravitational field, and,

* E-mail: m.shadmehri@gu.ac.ir; mmshadmehri@gmail.com

asymmetry of the H II regions can be attributed to the RT instability. In the optically thick and adiabatic regime, the RT growth rate is determined at the long-wavelength limit, however, it tends to a finite value when the radiation is close to the Eddington limit (JK). In short-wavelength limit the effect of the radiation field is negligible on the growth rate of the RT instability. Role of radiation field on the RT instability for a background state with a pure scattering opacity has been studied by Jiang et al. (2013) in both linear and nonlinear regimes. They solved the radiation hydrodynamic equations numerically with anisotropic radiation pressure in interface. The obtained growth rate of the RT instability exhibits a reduction in the presence of the radiation field and it decreases with radiation pressure. Results of Jiang et al. (2013) also showed that anisotropy of radiation plays an important in the nonlinear development of the RT instability.

Regarding to the importance of the magnetic fields, we extend the analysis of JK to the magnetized case with a uniform tangential magnetic field at both the upper and the lower flows. Basic equations are presented in section 2. We then investigate RT instability in the optically thin flows in section 3. A generalized dispersion relation including magnetic field and radiation is obtained. In section 3, our analysis of the magnetic RT instability is extended to the optically thick flows. We then conclude with astrophysical implications of our results in section 5.

2 PLASMA CONFIGURATION AND EQUATIONS

Basic equations of the Radiative Magnetohydrodynamic (RMHD) have been introduced and discussed by Stone et al. (1992) which are written in a comoving frame and are accurate up to $O(u/c)$, where u is the fluid velocity and c is the light speed. The momentum and the energy are exchanged between the material and the radiation. A similar set of the RMHD equations have also been implemented by Lowrie et al. (1999) and Blaes & Socrates (2003) in the equilibrium diffusion approximation. Upon neglecting gas self-gravity and assuming the flow is subject to a uniform gravity, the main RMHD equations are

$$\frac{D\rho}{Dt} + \rho \nabla \cdot \mathbf{u} = 0, \quad (1)$$

$$\rho \frac{D\mathbf{u}}{Dt} = -\nabla p_g + \rho \mathbf{g} + \frac{1}{4\pi} (\nabla \times \mathbf{B}) \times \mathbf{B} + \frac{\kappa_F \rho}{c} \mathbf{F}, \quad (2)$$

$$\rho \frac{D}{Dt} \left(\frac{E_r}{\rho} \right) = -\nabla \cdot \mathbf{F} - \nabla \mathbf{u} : \mathcal{P}_r - 4\pi \rho \kappa_p B_p - c \rho \kappa_E E_r, \quad (3)$$

$$\rho \frac{D}{Dt} \left(\frac{E_g + E_r}{\rho} \right) = -\nabla \cdot \mathbf{F} - \nabla \mathbf{u} : \mathcal{P}_r - p_g \nabla \cdot \mathbf{u}, \quad (4)$$

$$\frac{\rho}{c^2} \frac{D}{Dt} \left(\frac{\mathbf{F}}{\rho} \right) + \nabla \cdot \mathcal{P}_r = -\frac{\kappa_F \rho}{c} \mathbf{F}, \quad (5)$$

$$\frac{\partial \mathbf{B}}{\partial t} = \nabla \times (\mathbf{u} \times \mathbf{B}). \quad (6)$$

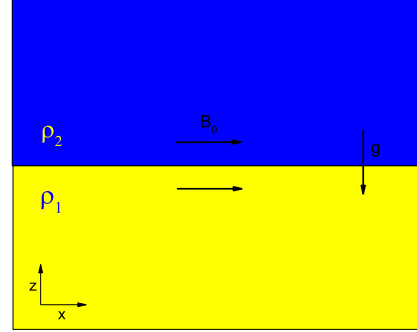


Figure 1. A fluid with the density ρ_2 is superposed on a lighter one, with density ρ_1 , such that the gravitational acceleration \mathbf{g} is perpendicular to the interface. An initial uniform magnetic field in parallel to the interface exists at both the upper and the lower layers.

Here, the Lagrangian derivative is denoted by $D/Dt \equiv \partial/\partial t + \mathbf{u} \cdot \nabla$ and \mathbf{u} is the velocity of the flow and E_r , F , \mathcal{P}_r and E_g , are the comoving radiation energy density, flux and stress tensor and the internal energy density, respectively and B_p is Planck function. The gas density, pressure and internal energy per unit volume are denoted by ρ , $p_g = \rho c_s^2$, and $E_g = p_g/(\gamma - 1)$, respectively. Furthermore, κ_F , κ_p and κ_E are the flux mean, Planck mean and energy mean opacities. Moreover, the isothermal sound speed is $c_s = \sqrt{k_B T/m}$, where k_B , T and m are the Boltzmann constant, the temperature and the mean mass per particle, respectively. The flow is assumed to be in the local thermal equilibrium. The above equations are closed with suitable relations for the equation of state, opacities and the Planck function and also a tensor variable Eddington factor f , i. e. $\mathcal{P}_r = f E_r$ (Stone et al. (1992)). In the following sections, we simplify the above basic equations under various approximations. We note that equation (4) can also be re-written as

$$\frac{DE_t}{Dt} + \mathcal{H}_t : \nabla \mathbf{u} = -\nabla \cdot \mathbf{F}. \quad (7)$$

This equation is actually equation (10) of JK. Here, we have $E_t = E_r + E_g$, $\mathcal{H}_t = E_t \mathcal{I}_3 + \mathcal{P}_t$, $\mathcal{P}_t = p_g \mathcal{I}_3 + \mathcal{P}_r$ and \mathcal{I}_3 is the 3×3 identity matrix.

The adopted geometry of our model is shown in Figure 1. In a Cartesian coordinates, we assume that the plane $z = 0$ specifies the interface between two fluids with different densities. We denote the physical quantities of the lower fluid ($z < 0$) by a subscript 1, and, those in the upper fluid ($z > 0$) are marked with a subscript 2. We assume that the initial magnetic field is uniform and tangent to the interface, i.e. $\mathbf{B} = B_0 \hat{x}$, whereas the gravitational acceleration is perpendicular to the interface, i.e. $\mathbf{g} = -g \hat{z}$.

3 ANALYSIS IN THE OPTICALLY THIN REGIME

We study the RT instability in an isothermal and optically thin system. We thereby suppose that both the upper and the lower fluids are kept at a fixed temperature and the radiation flux is assumed to be constant. Possible astrophysical implication of the present study are ionization fronts around H II regions (e.g., JK), the quasi-stellar object (QSO) clouds that may experience an intense central radiation force (e.g., Mathews & Blumenthal 1977b), and the radiation driven outflows in the ultraluminous infrared galaxies (Jiang et al. 2013).

The main equations for this regime are written as

$$\frac{D\rho}{Dt} + \rho \nabla \cdot \mathbf{u} = 0, \quad (8)$$

$$\rho \frac{D\mathbf{u}}{Dt} = -\nabla p_g + \rho \mathbf{g} + \frac{1}{4\pi} (\nabla \times \mathbf{B}) \times \mathbf{B} + \frac{\kappa_F \rho}{c} \mathbf{F}, \quad (9)$$

$$\frac{\partial \mathbf{B}}{\partial t} = \nabla \times (\mathbf{u} \times \mathbf{B}). \quad (10)$$

This set of equations is closed with the ideal gas equation of state, i.e. $p = k_B T \rho / m$.

3.1 Initial equilibrium state

We assume that the initial velocity of the flow is zero, and, the gas density and the radiation pressure are functions of the vertical coordinate z . Vertical component of the equation of motion leads to the following relation:

$$\frac{\partial p_g}{\partial z} = -\rho g + \frac{\kappa_F \rho}{c} F = -\rho g_{\text{eff}}. \quad (11)$$

where we suppose material with pure scattering opacity in both sides of the interface. The specific scattering κ_F and \mathbf{F} are assumed to be constant (JK, Jiang et al. 2013). So an effective gravitational acceleration is defined as $\mathbf{g}_{\text{eff}} = \mathbf{g} (1 - E)$ which is a constant, but may differ in the upper and lower layers, because the radiation flux may be different in the upper and lower layers. Here, the parameter E denotes the Eddington limit of the background state and is written as $E = (\kappa_F / cF) / (g)$. The above equation, therefore, can also be rewritten as

$$\frac{\partial p_g}{\partial z} = -\rho g (1 - E). \quad (12)$$

In the optically thin regime, we consider only electron scattering following previous studies (JK, Jiang et al. 2013). In our work, the Eddington parameter E is not dependent on the other parameters like α and β . We neglect role of radiation by setting $E = 0$. This particular case can be interpreted as a configuration in which either the opacity or radiation flux of one layer is much smaller than other layer. This approximation has already been implemented by JK in analyzing HII region around bright stars. In the optically thick regime, we can assume the opacity is a constant when the adiabatic approximation is used (JK). We note that when the gravitational force and the force of radiation are in balance, the Eddington limit is the maximum

luminosity a body (such as a star) can achieve while keeping the system in equilibrium. For example, if radiation of a star exceeds the Eddington luminosity, the surface layers are no longer in equilibrium and one can expect a very intense radiation-driven stellar wind from its outer layers. As we mentioned earlier, the initial magnetic field B_0 is assumed to be uniform and tangent to the interface. The initial magnetic field is the same at both upper and lower layers because of the continuity of the magnetic pressure. But the density and the temperature are different at two sides of the interface.

3.2 Linear perturbations

Using the above initial equilibrium state, we can now perturb each physical quantity as $\chi \equiv \chi_0 + \chi'$, where the perturbed quantity is much smaller than the equilibrium state, i.e. $|\chi'| \ll |\chi_0|$. Upon substituting linear perturbations into equations 8, 9, 10 and the equation of state, a set of linear differential equations is obtained such that one can study their time-evolution as $\chi'(z, x, t) = \chi'(z) \exp(\omega t + ik_x x)$, where the primed quantities are the amplitude of the perturbations, ω is the growth rate of the instability, and, k_x is wavenumber of perturbations. We note that with this form of time-dependence part of the perturbations, real values of ω imply exponential growth which then correspond to the unstable modes. We then arrive to the following linearized differential equations:

$$\omega \rho' + u'_z \frac{\partial \rho}{\partial z} + \rho (ik_x u'_x + \frac{\partial u'_z}{\partial z}) = 0, \quad (13)$$

$$\rho \omega u'_x = -ik_x p', \quad (14)$$

$$\rho \omega u'_z = -\frac{\partial p'}{\partial z} - \rho' g_{\text{eff}} + \frac{B_0^2}{4\pi \omega} (\frac{\partial^2 u'_z}{\partial z^2} - k_x^2 u'_z), \quad (15)$$

$$p' = c_s^2 \rho'. \quad (16)$$

Note that equilibrium state is denoted by quantities without subscript, for simplicity. After straightforward mathematical manipulations, we obtain

$$\frac{\partial^2 u'_z}{\partial z^2} - \frac{g_{\text{eff}}}{c_s^2} (\frac{\omega^2}{\omega^2 + v_A^2 q^2}) \frac{\partial u'_z}{\partial z} - q^2 (\frac{\omega^2 + v_A^2 k_x^2}{\omega^2 + v_A^2 q^2}) u'_z = 0, \quad (17)$$

where $q^2 = \omega^2 / c_s^2 + k_x^2$, and, v_A is Alfvén speed, i.e. $v_A = B_0 / \sqrt{4\pi \rho}$. This is an ordinary linear differential equation with constant coefficients and its general solution can be written as,

$$u'_z = A_1 \exp(s_+ z) + A_2 \exp(s_- z), \quad (18)$$

and the parameters s_+ and s_- are obtained as,

$$s_{\pm} = \frac{g_{\text{eff}} \omega^2}{2c_s^2 (\omega^2 + v_A^2 q^2)} \pm \sqrt{\left[\frac{g_{\text{eff}} \omega^2}{2c_s^2 (\omega^2 + v_A^2 q^2)} \right]^2 + q^2 \left(\frac{\omega^2 + v_A^2 k_x^2}{\omega^2 + v_A^2 q^2} \right)}. \quad (19)$$

A general dispersion relation is obtained by imposing the following boundary conditions at the interface: (1) The

perturbations must tend to zero as z goes to the infinity; (2) The z -component of the velocity is continuous at the interface; (3) The total pressure, including radiation, magnetic and gas pressures must be continuous at the interface. Using these boundary conditions and the fact that one of the roots is always positive and the other one is negative, we obtain $u'_z = A_2 \exp(s_- z)$ for the upper layer ($z > 0$), and, $u'_z = A_1 \exp(s_+ z)$ for the lower layer ($z < 0$). Also, continuity of the total pressure at the interface is written as

$$(p'_g + p'_m - \rho g_{\text{eff}} \zeta)|_{0+} = (p'_g + p'_m - \rho g_{\text{eff}} \zeta)|_{0-}, \quad (20)$$

where p'_m is the perturbed magnetic pressure, i.e. $p'_m = -(B_0^2/4\pi\omega)(\partial u'_z/\partial z)$ and $\zeta = u'_z/\omega$. Dispersion relation, therefore, is obtained as

$$\begin{aligned} & \frac{\rho_2}{\omega^2 + k_x^2 c_{s_2}^2} (\omega^2 c_{s_2}^2 s_- + g_{\text{eff}2} k_x^2 c_{s_2}^2) + v_{A_2}^2 \rho_2 s_- - \\ & - \frac{\rho_1}{\omega^2 + k_x^2 c_{s_1}^2} (\omega^2 c_{s_1}^2 s_+ + g_{\text{eff}1} k_x^2 c_{s_1}^2) - v_{A_1}^2 \rho_1 s_+ = 0, \quad (21) \end{aligned}$$

and this equation can be written as

$$\begin{aligned} & \frac{1}{x^2 + y^2 \mu^2} (\alpha x^2 S_- + \alpha(1 - E_2)y^2 \mu^2) - \\ & - \frac{1}{x^2 + y^2} (x^2 S_+ + (1 - E_1)y^2) + \beta_2^2 \alpha S_- - \beta_1^2 S_+ = 0. \quad (22) \end{aligned}$$

Here, the dimensionless parameters x, y, S_-, S_+, β_1 , and β_2 are defined as

$$\begin{aligned} x &= \frac{\omega}{g} c_{s_1}, \quad y = \frac{k_x}{g} c_{s_1}^2, \quad \alpha = \frac{\rho_2}{\rho_1}, \quad \mu = \frac{c_{s_2}}{c_{s_1}}, \\ \beta_2 &= \frac{v_{A_2}}{c_{s_2}}, \quad \beta_1 = \frac{v_{A_1}}{c_{s_1}}, \quad S_- = \frac{s_-}{g} c_{s_2}^2, \quad S_+ = \frac{s_+}{g} c_{s_1}^2. \quad (23) \end{aligned}$$

We note that not all the above defined dimensionless parameters are independent. In fact, pressure continuity implies that the parameters of α and μ are not independent and we have $\alpha\mu^2 = 1$. Furthermore, continuity of magnetic pressure implies that $\beta_1 = \beta_2$. Also, we have

$$\begin{aligned} S_- &= \frac{(1 - E_2)x^2}{2(x^2 + \beta_2^2 x^2 + \beta_2^2 \mu^2 y^2)} - \left[\frac{(1 - E_2)x^2}{2(x^2 + \beta_2^2 x^2 + \beta_2^2 \mu^2 y^2)} \right]^2 \\ &+ (x^2 \mu^2 + y^2 \mu^4) \left(\frac{x^2 + \beta_2^2 \mu^2 y^2}{x^2 + \beta_2^2 x^2 + \beta_2^2 \mu^2 y^2} \right)^{1/2}, \quad (24) \end{aligned}$$

$$\begin{aligned} S_+ &= \frac{(1 - E_1)x^2}{2(x^2 + \beta_1^2 x^2 + \beta_1^2 y^2)} + \left[\frac{(1 - E_1)x^2}{2(x^2 + \beta_1^2 x^2 + \beta_1^2 y^2)} \right]^2 \\ &+ (x^2 + y^2) \left(\frac{x^2 + \beta_1^2 y^2}{x^2 + \beta_1^2 x^2 + \beta_1^2 y^2} \right)^{1/2}. \quad (25) \end{aligned}$$

Equation (22) is our non-dimensional dispersion relation for analyzing the magnetic RT instability in an optically thin medium which can be solved numerically. Before presenting our numerical analysis of this equation, however, it is possible to obtain analytical solutions for a few simplified cases as we show in the next subsections.

3.3 Dispersion relation in simplified cases

If we ignore radiation and magnetic fields, we can set $E_1 = E_2 = 0$ and $\beta_1 = \beta_2 = 0$ into equation (22), and thereby, the classical nonmagnetic dispersion relation is obtained which is the same as equation (16) of Shivamoggi (2008) for a similar configuration for $\mu = 1$. Moreover, the incompressible limit is obtained, if the sound speed in both the upper and the lower fluids tends to infinity. We then obtain

$$x^2 = \frac{\alpha - 1}{\alpha + 1} y, \quad (26)$$

which is in agreement with the results of Chandrasekhar (1961) for a similar problem. It is found that the system is prone to the RT instability, if we have $\rho_2 > \rho_1$, and, the compressibility does not change this criteria for the onset of instability. As the wavelength of the perturbations becomes longer, however, reduction of the growth rate due to the compressibility becomes more noticeable. Furthermore, Chandrasekhar (1961) presented a linear analysis of the incompressible magnetic RT instability including a uniform magnetic field. It turns out a uniform tangential magnetic field slows down the growth rate of the RT instability. The growth rate for the unstable modes with wavenumber k_x parallel to the magnetic field lines is given by the following equation

$$\begin{aligned} & \frac{1}{x^2 + y^2 \mu^2} (\alpha x^2 S_- + \alpha y^2 \mu^2) - \\ & - \frac{1}{x^2 + y^2} (x^2 S_+ + y^2) + \beta_2^2 \alpha S_- - \beta_1^2 S_+ = 0, \quad (27) \end{aligned}$$

and if the sound speed tends to infinity, the growth rate for the incompressible case with $\beta_1 = \beta_2 = \beta$ and $\mu = 1$ is obtained, i.e.

$$x^2 = \frac{\alpha - 1}{\alpha + 1} y - \frac{2}{\alpha + 1} \beta^2 y^2, \quad (28)$$

which is consistent with the previous studies (e.g., Chandrasekhar 1961).

Figure 2 shows growth rate of the unstable perturbations as a function of the wavenumber based on the roots of equation (27) for $\mu = 0.45$ and $\alpha = 5$ and different values of β where $\beta_1 = \beta_2 = \beta$. The compressible and incompressible cases are shown by solid and dashed lines, respectively. Magnetic field has a stabilizing role in the RT instability by reducing the growth rate in comparison to the nonmagnetic case. In the presence of magnetic field, maximum growth rate occurs for a particular wavenumber, whereas in the nonmagnetic case, the growth rate increases with increasing the wavenumber. The critical wavenumber corresponding to the fastest growth rate reduces as the magnetic field becomes stronger. Although Figure 2 corresponds to a particular set of the input parameters, we also found a similar behavior for the other set of the input parameters. Role of the radiation field in RT instability, however, is explored by setting $\beta_1 = 0$ and $\beta_2 = 0$ in equations (22), (23) and (25). Then, the dispersion relation can be written as

$$\begin{aligned} & \frac{1}{x^2 + y^2 \mu^2} (\alpha x^2 S_- + \alpha(1 - E_2)y^2 \mu^2) - \\ & - \frac{1}{x^2 + y^2} (x^2 S_+ + (1 - E_1)y^2) = 0. \quad (29) \end{aligned}$$

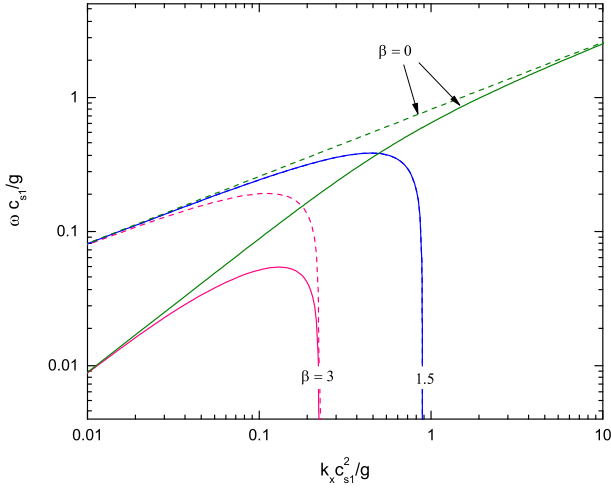


Figure 2. Dimensionless growth rate of the magnetic RT instability in the compressible case is obtained by solving the full dispersion relation (27) for $\mu = 0.45$, $\alpha = 5$, $\beta_1 = \beta_2 = \beta$, and different values of β (solid lines), however, dashed lines show growth rate of the instability in the incompressible case.

This equation is the same as equation (74) of JK. In Figure 3 the dashed lines indicate unstable growth rates as a function of the wavenumber for $E_1 = 0$ and different values of E_2 . The system is unstable when the effective gravity is negative. In agreement with previous studies (Jiang et al. 2013, JK), we also find that growth rate of the instability decreases with radiation pressure. Figure 4 displays growth rate of the instability for $E_2 = 0$ and different values of E_1 . Here, the radiation force is assumed to be against the gravity (for having a unstable state). Therefore, the input parameter E_1 is adopted positive.

Up to now we have investigated radiative RT instability and magnetic RT instability separately. Using Equations (22), (23) and (25), we can explore magnetic radiative RT instability in the optically thin regime. Figure 3 shows growth rate of the RT instability including both magnetic and radiative effects as a function of the wavenumber of the perturbations for $\beta_1 = \beta_2 = \beta = 3$, $\mu = 0.45$, $\alpha = 5$ and, $E_1 = 0$ (solid lines). In order to make easier comparison, we also show growth rate of the non-magnetic radiative RT instability by dashed lines. Each curve is labeled by the value of the corresponding Eddington parameter E_2 . Moreover, dotted line represents a case with $E_1 = 0$ which tends to the classical RT instability. Figure 4 is similar to Figure 5, but for $E_2 = 0$. This configuration may exist in boundary of a radiation-driven H II region. Growth rate of the RT instability reduces With increasing β . Magnetic fields strongly suppress the instability at long wavelengths, however, a radiation field reduces growth rate of the instability at all wavelengths. In the presence of the magnetic field, there is always a characteristic wavelength at which growth rate of the RT instability reaches to a maximum value. With increasing the Eddington limit of the background state E which implies a stronger radiation field, the wavelength of the fastest growing mode shifts to the longer wavelengths and the growth

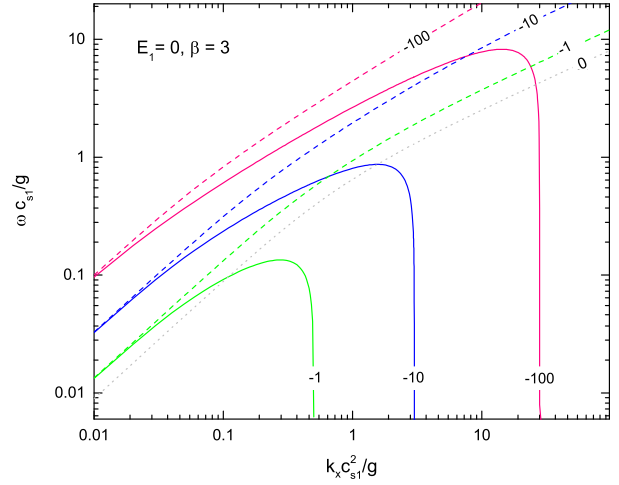


Figure 3. Growth rate of the magnetic radiative RT instability in the optically thin regime is shown by solid lines for $\beta = 3$, $\mu = 0.45$, and, $\alpha = 5$. Each curve is labeled by the corresponding value of E_2 . The dashed lines are radiative RT instability for the same parameters.

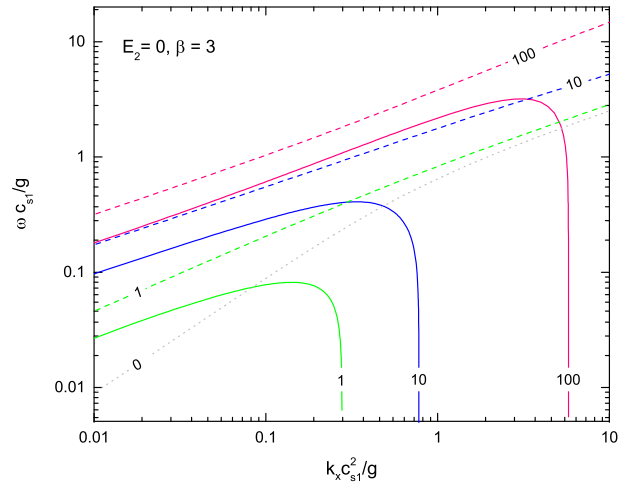


Figure 4. Same as Figure 3, but for $E_2 = 0$ and each curve is labeled by the corresponding value of E_1 .

rate of the instability reduces. In other words, a radiation field in the optically thin regime has a stabilizing role on the magnetic RT instability.

4 ANALYSIS IN THE OPTICALLY THICK REGIME

We now analyze RT instability in the optically thick regime. Following JK approach in which the radiation field is assumed to be Planckian with $T_r = T_g = T$, and the comoving

radiation pressure tensor to be isotropic, i.e. $\mathcal{P}_r = (E_r/3)\mathcal{I}_3$ and $E_r = aT^4$, we can simplify equation (4) as

$$-\frac{\kappa_F \rho}{c} \mathbf{F} \approx \nabla p_r, \quad (30)$$

provided that photon mean free path, i.e. $1/(\kappa_F \rho)$, is smaller than the wavelength of the perturbations and the characteristic length scale of the system. Here, the Planck and energy opacities are assumed to be equal and constant. Thus, equations (2) and (3) become

$$\rho \frac{D\mathbf{u}}{Dt} = -\nabla p_t + \rho \mathbf{g} + \frac{1}{4\pi} (\nabla \times \mathbf{B}) \times \mathbf{B}, \quad (31)$$

$$\frac{DE_t}{Dt} + (E_t + p_t) \nabla \cdot \mathbf{u} = -\nabla \cdot \mathbf{F}. \quad (32)$$

where $p_t = p_g + p_r$.

4.1 Initial equilibrium state

As before we must specify the initial configuration which is supposed to be in thermal and mechanical equilibrium. As we now argue, however, the system can not fulfill thermal and mechanical equilibrium conditions simultaneously unless some further assumptions are implemented. Since the initial state is in mechanical equilibrium and the upper and the lower layers have different densities, their temperatures can not be the same. Thermal equilibrium, however, implies that both layers have the same temperature. In order to resolve this contradiction, JK proposed that one layer is optically thin and the second layer is optically thick. They also assumed that the system is adiabatic. In the optically thin regime, where opacity on one or both sides of the interface is negligible, continuity of E_r holds on whereas T_g is independent of E_r . There are, however, further alternative ways to specify background state self-consistently. Jiang et al. (2013), for instance, argued that even when the background state is not strictly in thermal equilibrium, its evolution affects subsequent thermal evolution very slightly so long as thermal time-scale is much longer than the instability time-scale. Under these circumstances, therefore, the initial configuration can be imagined to be in thermal equilibrium for exploring RT instability. Jiang et al. (2013) constructed an initial state with zero absorption opacity and effectively infinite thermal time-scale. As we mentioned earlier, JK assumed that one side of interface is in the adiabatic regime, and the other side is in the optically thin regime. Here, we follow JK assumptions for specifying the initial equilibrium state which are applicable to some astrophysical systems.

The momentum and the energy equations are written as

$$\frac{\partial p_g}{\partial z} = -\rho g(1 - E), \quad (33)$$

$$\frac{\partial E_t}{\partial t} = -\nabla \cdot \mathbf{F} = 0. \quad (34)$$

where $\mathbf{F} = (-c/3\kappa_F \rho) \nabla E_r$. Equation (34) is written based on the radiative equilibrium assumption. The parameter E represents the Eddington limit of the background state. We note that the introduced parameter E is then replaced by

E_1 and E_2 for the lower and the upper layers, respectively. Also, we have

$$\frac{dT}{dz} = \frac{T}{4p_r} \frac{dp_r}{dz} = \frac{T}{4p_r} (-\rho g E). \quad (35)$$

Introducing ratio of the radiation pressure to the gas pressure as $r = p_r/p_g$, we can then write

$$\frac{\partial \rho}{\partial z} = \frac{\rho g}{c_s^2} (E - 1 + \frac{E}{4r}), \quad (36)$$

and

$$\frac{\partial E_t}{\partial z} = \rho g \left(\frac{E - 1}{\gamma - 1} - 3E \right). \quad (37)$$

We note that the Eddington limit parameter E is a fixed input parameter, however, the parameter r is not a constant under our imposed conditions.

4.2 Linear perturbations

After deriving the above equilibrium solutions, we can now linearly perturb RMHD equations. Following JK, we also apply *adiabatic approximation* by which we mean perturbed energy flux is neglected. It means that we require $F' \ll E_t u'$. Using this approximation, we can assume that the opacity is a constant. Therefore, the parameter E becomes a constant which is actually our implemented assumption. This parameter, however, may be different in the upper and lower layers. We thereby arrive to the following equations:

$$\omega \rho' + u'_z \frac{d\rho}{dz} + \rho (ik_x u'_x + \frac{\partial u'_z}{\partial z}) = 0, \quad (38)$$

$$\rho \omega u'_z = -\frac{\partial p'_t}{\partial z} - \rho' g - \frac{B_0}{4\pi} \left(\frac{\partial b'_x}{\partial z} - ik_x b'_z \right), \quad (39)$$

$$\rho \omega u'_y = \frac{B_0}{4\pi} (ik_x b'_y), \quad (40)$$

$$\rho \omega u'_x = -ik_x p'_t, \quad (41)$$

$$\omega \left(\frac{1}{\gamma - 1} p'_g + 3p'_r \right) + \mathbf{u}' \cdot \nabla E_t - \frac{(E_t + p_t)}{\rho} (\omega \rho' + u'_z \frac{d\rho}{dz}) = 0, \quad (42)$$

$$\frac{p'_g}{p_g} = \frac{\rho'}{\rho} + \frac{p'_r}{4p_r}, \quad (43)$$

$$p'_t = p'_g + p'_r, \quad (44)$$

$$\omega b'_x = -B_0 \left(\frac{\partial u'_z}{\partial z} \right), \quad (45)$$

$$\omega b'_y = B_0 (ik_x) u'_y, \quad (46)$$

$$\omega b'_z = B_0 (ik_x) u'_z, \quad (47)$$

$$ik_x b'_x + \frac{\partial b'_z}{\partial z} = 0. \quad (48)$$

As before, we assume all the perturbed quantities are proportional to $\exp(\omega t + ik_x x)$, and the above equations after lengthy but straightforward calculations reduce to the following equations:

$$\omega \rho' + u'_z \frac{d\rho}{dz} + \rho \left(\frac{k_x^2}{\omega \rho} p'_t + \frac{\partial u'_z}{\partial z} \right) = 0, \quad (49)$$

$$\rho \omega u'_z = -\frac{\partial p'_t}{\partial z} - \rho' g + \frac{B_0^2}{4\pi\omega} \left(\frac{\partial^2 u'_z}{\partial z^2} - k_x^2 u'_z \right), \quad (50)$$

$$\frac{p'_t}{\rho g} C = \frac{\rho'}{\rho} + \frac{gB}{c_s^2} \frac{u'_z}{\omega}, \quad (51)$$

where parameters B and C depend on the input parameters which specify the initial configuration of the system, i.e.

$$B = \frac{1}{16r^2 + 20r + \frac{\gamma}{\gamma-1}} [16r^2(E-1) + r(24E-8) + \quad (52)$$

$$+ E(5 + \frac{\gamma}{\gamma-1}) - 1 + \frac{E\gamma}{4r(\gamma-1)}], \quad (53)$$

$$C = \frac{12r + \frac{1}{\gamma-1}}{16r^2 + 20r + \frac{\gamma}{\gamma-1}}. \quad (54)$$

We now obtain ρ' from equation (51) and substitute it into equations (49) and (50):

$$\frac{\partial u'_z}{\partial z} = \frac{g}{c_s^2} C u'_z - \frac{1}{\rho\omega} \left(\frac{\omega^2 C}{c_s^2} + k_x^2 \right) p'_t, \quad (55)$$

$$\frac{\partial p'_t}{\partial z} = \left(\frac{\rho g^2}{c_s^2 \omega} B - \rho\omega \right) u'_z - g \frac{C}{c_s^2} p'_t + \frac{\beta^2 \rho c_s^2}{\omega} \left(\frac{\partial^2 u'_z}{\partial z^2} - k_x^2 u'_z \right). \quad (56)$$

Substituting $\partial u'_z / \partial z$ from equation (55) into equation (56), this equation becomes

$$\begin{aligned} & - \left(A \frac{\omega^2 c_s^2}{g^2} + \beta^2 \frac{k_x^2 c_s^4}{g^2} \right) \frac{\partial p'_t}{\partial z} + \rho\omega \left(G - \left(\frac{\omega}{g} c_s \right)^2 - \beta^2 \frac{k_x^2}{g^2} c_s^4 \right) u'_z - \\ & - \frac{g}{c_s^2} \left[I \frac{\omega^2}{g^2} c_s^2 - \beta^2 (E-1) + \frac{E}{4r} \right] \frac{k_x^2}{g^2} c_s^4 p'_t + \\ & + \beta^2 \rho c_s^2 C \frac{\omega}{g} \frac{\partial u'_z}{\partial z} = 0, \quad (57) \end{aligned}$$

where

$$A = \beta^2 C + 1, \quad (58)$$

$$I = C - \beta^2 (E-1)C - \beta^2 H, \quad (59)$$

$$H = \frac{12 - C(32r + 20)}{16r^2 + 20r + \frac{\gamma}{\gamma-1}} (E + r(E-1)), \quad (60)$$

$$G = B + \beta^2 \left(\frac{CE}{4r} - H \right). \quad (61)$$

Note that the parameters C , c_s , and, r are not constant and their spatial dependence are obtained from the initial conditions, i.e. $\partial r / \partial z = -(g/c_s^2)(E + x(E-1))$.

Now we consider perturbations which are actually localized at the interface. This means that we perform a WKB analysis of the vertical modes which it enables us to eliminate the first order derivative terms. This condition is referred by JK as *adiabatic approximation*. By assuming that quantities p'_t and u'_z are proportional to $\exp(sz)$, then equations (55) and (57) become

$$\frac{g}{c_s^2} \left(\frac{s}{g} c_s^2 - C \right) u'_z + \frac{1}{\rho\omega} \left(\frac{\omega^2}{c_s^2} C + k_x^2 \right) p'_t = 0, \quad (62)$$

and

$$\rho\omega \left(G - \frac{\omega^2 c_s^2}{g^2} - \beta^2 \frac{k_x^2 c_s^4}{g^2} + \frac{\beta^2 c_s^2}{g} C s \right) u'_z - \quad (63)$$

$$- \frac{g}{c_s^2} \left[\frac{c_s^2}{g} s \left(A \frac{\omega^2 c_s^2}{g^2} + \beta^2 \frac{k_x^2 c_s^4}{g^2} \right) + I \frac{\omega^2 c_s^2}{g^2} - \beta^2 Z \frac{k_x^2 c_s^4}{g^2} \right] p'_t = 0,$$

where $Z = E - 1 + E/4r$. From equations (62) and (63) by introducing $S = (c_s^2/g)s$, we obtain

$$S^2 (A\omega^2 + \beta^2 c_s^2 k_x^2) - S(K\omega^2 + \beta^2 Z c_s^2 k_x^2) - C(I\omega^2 -$$

$$- \beta^2 Z c_s^2 k_x^2) + \left(G - \frac{\omega^2 c_s^2}{g^2} - \beta^2 \frac{k_x^2 c_s^4}{g^2} \right) (\omega^2 C + c_s^2 k_x^2) = 0, \quad (64)$$

where $K = C - I$. Equation (64) is solved numerically and a positive root, S_- , and a negative root, S_+ , are obtained. Using these roots, the general solution can be written as equation (18). Then, we apply boundary conditions. Continuity of the pressure at the interface is written as

$$\left(p'_t + p'_m - \rho g \zeta \right)_{z=0^+} = \left(p'_t + p'_m - \rho g \zeta \right)_{z=0^-}, \quad (65)$$

where p'_t is obtained from equation (55) as follows

$$p'_t = \rho\omega \frac{C g u'_z / c_s^2 - \partial u'_z / \partial z}{\omega^2 C / c_s^2 + k_x^2}, \quad (66)$$

and p'_m is given by

$$p'_m = -\frac{B_0^2}{4\pi\omega} \frac{\partial u'_z}{\partial z}. \quad (67)$$

Finally, the dispersion relation is obtained from equation (65) and by imposing boundary conditions, i.e.

$$\begin{aligned} (S_-) & \left(\frac{\alpha\omega^2}{C_2\omega^2 + c_{s_2}^2 k_x^2} + \alpha\beta_2^2 \right) + \left(\frac{\alpha c_{s_2}^2 k_x^2}{C_2\omega^2 + c_{s_2}^2 k_x^2} \right) - \\ & - (S_+) \left(\frac{\omega^2}{C_1\omega^2 + c_{s_1}^2 k_x^2} + \beta_1^2 \right) - \left(\frac{c_{s_1}^2 k_x^2}{\omega^2 C_1 + c_{s_1}^2 k_x^2} \right) = 0, \quad (68) \end{aligned}$$

where S_- and S_+ are obtained from equation (64) for regions 2 and 1, respectively. We note that in the absence of magnetic field (i.e., $\beta = 0$), equation (68) reduces to equation (74) of JK, i.e.

$$\frac{\alpha}{(x^2 C_2 + y^2 \mu^2)} (y^2 \mu^2 -$$

$$-x^2 \sqrt{C_2(C_2 - B_2) + x^2 C_2 \mu^2 - \frac{y^2 \mu^2}{x^2} B + y^2 \mu^4} = \quad (69)$$

$$= \frac{1}{(x^2 C_1 + y^2)} (y^2 + x^2 \sqrt{C_1(C_1 - B_1) + x^2 C_1 - \frac{y^2}{x^2} B + y^2}).$$

Equation (68) is a dispersion relation when two sides of interface are adiabatic. In addition to assuming that one side (e.g., region 1) is in the optically thin regime, we also suppose that $\rho_2 \gg \rho_1$ and $c_{s2} \ll c_{s1}$ and the magnetic field is not strong. Upon applying these simplifying assumptions, therefore, Equation (68) reduces to

$$(S_-) \left(\frac{\omega^2}{C_2 \omega^2 + c_{s2}^2 k_x^2} + \beta_2^2 \right) + \left(\frac{c_{s2}^2 k_x^2}{C_2 \omega^2 + c_{s2}^2 k_x^2} \right) = 0. \quad (70)$$

Equation (70) is our main equation that we plan to investigate it in more detail. In the long-wavelength limit, we have

$$\omega^2 = \left(\frac{g}{c_{s2}} \right)^2 (G_2 - I_2). \quad (71)$$

If we set $\beta_2 = 0$, JK relation (78) is recovered. The growth rate increases with magnetic field strength. A critical wavenumber is obtained by assuming that $\omega = 0$. Thus, the critical wavenumber becomes

$$k_x^2 = \left(\frac{g^2}{c_{s2}^4} \right) (C_2 Z_2 + \frac{G_2}{\beta_2^2} + \frac{Z_2}{\beta_2^2} + \frac{1}{\beta_2^4}). \quad (72)$$

Perturbations with a wavelength longer than critical wavelength are completely suppressed in the presence of the magnetic fields. In the short-wavelength limit, however, the growth rate tends to equation (71).

Equation (70) can be solved numerically for a given set of the input parameters. Figure 5 shows the growth rates of the RT instability for different values of parameter β_2 . Compressible RT instability is also shown by dotted line. Growth rate of the instability decreases because of considering magnetic fields. We can also determine the fastest growing mode which is an important quantity. Before doing so, however, we discuss about validity of our results and the applied assumptions.

4.3 Validity of the Approximations

We now discuss about validity of the imposed assumptions in the optically thick regime. The requirement of the optically thick regime implies that $\tau = L/\lambda \gg 1$, where L is the characteristic size of the system, i.e. $L = \min(1 + r, r/E)c_s^2/g$, and $\lambda = 1/\kappa_F \rho$ is the photon mean free path. Thus, it must be smaller than the wavelength of the perturbations and the characteristic length scale of the system. Now we propose to consider evanescence condition that by which we have $1/s < L$, where s is proportional to the perturbation in the z direction. Note that dimensionless parameter s is defined in equation (23). We can obtain s from the equation (70):

$$s_- = -g \frac{k_x^2}{\omega^2 + \beta_2^2 C_2 \omega^2 + v_{A2}^2 k_x^2}. \quad (73)$$

This term becomes negative, because the perturbations are finite as z tends to the infinity in the positive direction of

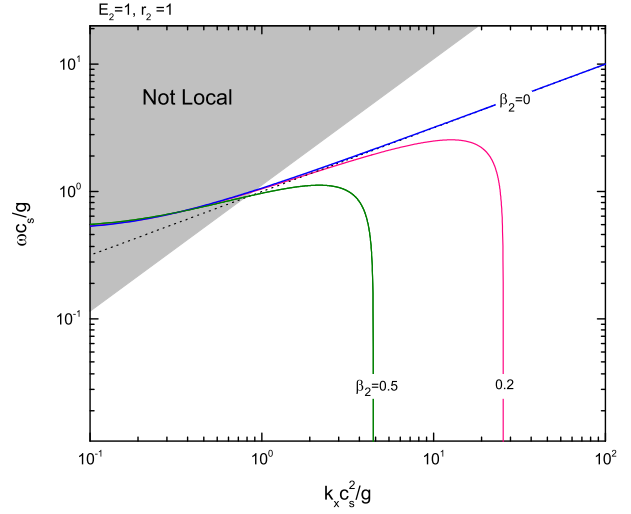


Figure 5. Growth rate of the adiabatic, optically thick radiative RT instability in the presence of magnetic field. Solid lines represent cases with different parameter β_2 . A case without magnetic field is also shown. Dotted line shows growth rate of the compressible RT instability. The gray region displays the evanescence constraint (the decay of perturbations on the length-scales smaller than the background equilibrium scale height) is violated according to equation (75).

the z axis. Now we can write the evanescence condition as:

$$\frac{\omega}{k_x} < c_s \sqrt{\frac{\min(1 + r_2, r_2/E_2) - \beta_2^2}{1 + \beta_2^2 C_2}}, \quad (74)$$

and in the dimensionless form, it becomes

$$\frac{x}{y} < \sqrt{\frac{\min(1 + r_2, r_2/E_2) - \beta_2^2}{1 + \beta_2^2 C_2}}. \quad (75)$$

If we set $\beta_2 = 0$, the above relation reduces to equation (76) of JK. The invalid region based on equation (75) is shown as a shaded area in Figure 5 for $\beta_2 = 0.5, 0.45$ and $E_2 = r_2 = 1$. The obtained results are valid over a wider range of the input parameters with increasing parameter β_2 . As for the adiabatic approximation, we must have $F_z' \ll E_t v_z'$ to ignore of the perturbation of the radiation flux. Since we have $p_r' = -\xi(dp_r/dz) = E\rho g\xi$ and considering linearized equation of the radiation flux, we obtain

$$F_z' > \frac{-c}{\kappa\rho} \frac{dp_r'}{dz} = \frac{-c}{\kappa\rho} s p_r' = -s F_0 \xi, \quad (76)$$

and so,

$$\frac{F_0}{E_t} \ll -\frac{\omega}{s} = \frac{\omega}{gk_x} (\omega^2 + v_A^2 (\omega^2 \frac{C_2}{c_s^2} + k_x^2)). \quad (77)$$

This relation shows that the adiabatic approximation at long and small wavelengths is reliable. Considering equations (74) and (77) for a given value of F_0/E_t , since the calculations do not depend on F_0/E_t , we can conclude that our results are valid. For strong magnetic fields, however, we note that the evanescence condition is violated.

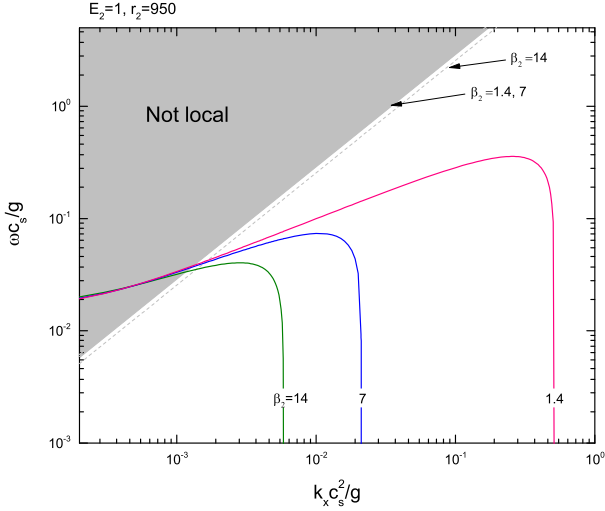


Figure 6. Same as Figure 5, but for the parameters $E_2 = 1$, $r_2 = 950$.

5 ASTROPHYSICAL IMPLICATIONS: RADIATIVE BUBBLES IN THE MASSIVE STAR FORMING REGIONS

We did a detailed analysis of the radiative RT instability in the presence of magnetic field. Our parameter study shows that magnetic fields are able to significantly modify unstable radiative RT modes which have already been studied by JK. We now present astrophysical implications of our study. JK investigated radiative RT instability in the massive star forming regions without considering role of the magnetic field. Since radiation of a young star can be stronger than its gravitational force near the Eddington limit, further gas accretion onto the star can be prevented. Thus, the net force on the gas component is outward which pushes the gas toward outer regions. Under these circumstances, however, the interface between a low-density bubble and high-density shell that is generated from swept gas is prone to the RT instability. Even with a strong central radiation source, further gas accretion is possible as a result of non-linear growth of the RT instability (Krumholz et al. 2009). JK studied stability of this interface subject to RT instability in an extreme condition where the flow is near the Eddington limit. They found that linear growth time-scale of RT instability is less than 1000 years which is quite short compared to the star formation time-scale which is approximately of order 10^5 years.

Observational evidences, however, indicate that magnetic fields may play a significant dynamical role in the photon bubbles of the star forming regions. Zeeman measurements show that the strength of the magnetic fields in these systems is about 0.01 – 0.6 G (Sarma et al. 2002; Vlemmings et al. 2006). Turner et al. (2007) investigated radiative bubbles in the circumstellar envelopes of young massive stars with a magnetic field of around 0.1 G.

We now re-examine RT instability in the *magnetized* radiative bubbles. The central massive star is assumed to have a mass $M_* = 100 M_\odot$, and, its luminosity is $L_* = 10^5$

L_\odot . So all the above parameters are calculated for the shell. At the edge of the bubble, we assume that physical quantities are $\rho = 10^{-16} \text{ g cm}^{-3}$, $T = 1100\text{K}$, $\gamma = 7/5$ (for molecular hydrogen), and, the mean mass per particle is $m = 2.33m_H$. Then, the gas sound speed becomes $c_s \approx 2 \text{ km s}^{-1}$. In the dense gas, we assume that $E_2 \approx 1$ and $r_2 = 950$ (JK) and consider the strength of the magnetic field to be about a few tens milli-Gauss. Given all the input parameters, one can easily solve equation (70) numerically. In Fig. 6, we have $B_0 = 10, 50, 100 \text{ mG}$ which then imply that $\beta_2 = 1.4, 7, 14$. The minimum bubble-growth time, therefore, becomes about 180 kyr and 900 kyr for $\beta_2 = 1.4$ and 7, respectively. This time-scale is a few times longer than formation timescale. The corresponding wavelength, furthermore, is about 10^5 AU which is roughly ten times larger than bubble size. The allowed region according to equations (74) and (77) is shown as a shaded area in Fig. 6. For $\beta_2 = 14$ this area becomes slightly larger than a case with a lower β_2 . So, we can verify that our results are reliable for this range of the magnetic field. If the central mass is assumed to be 10 solar masses, the growth time would be ten times longer than what we just obtained. Thus, growth rate of instability decreases, when a central star with a lower mass is considered. Our stability analysis is a variant of the magnetic buoyancy instability in which magnetic field lines and the direction of the perturbations are in parallel. Importance of the magnetic buoyancy instability in the Galactic disc (including cosmic ray component) to explain formation of the molecular clouds has been emphasized by Parker (1966) and further developments towards understanding nonlinear evolution of this instability are based on the direct numerical simulations (e.g., Matsumoto et al. 1993; Basu et al. 1997; Hanasz & Lesch 2003; Rodrigues et al. 2016). However, we did not explore magnetic buoyancy instability in the presence of a radiation field when the perturbations are perpendicular to the magnetic field vector. In Figure 6, for instance, the gas and magnetic pressures are comparable when magnetic field strength is $B_0 = 10 \text{ mG}$, whereas magnetic pressure becomes much larger than the gas pressure for a case with $B_0 = 100 \text{ mG}$. It deserves further study to explore stability of this strongly magnetized configuration in the presence of a radiation field subject to the perturbations perpendicular to the magnetic field lines because the instability may become so efficient that gas can get to the star.

6 CONCLUSIONS

In this study, we studied radiative and magnetic RT instability in the linear regime. In the absence of radiation or magnetic field, our dispersion equation reduces to results of the previous studies (e.g., JK), however, we found new features of the instability when radiation and magnetic effects are significant. In the context of massive star formation, radiation pressure of a young central star is able to prevent further accretion of mass unless some mechanisms like RT instability at the edge of the radiation-driven bubble around the star provide channels of mass accretion onto it (e.g., Rosen et al. 2016; Klassen et al. 2016). Linear development of radiative RT instability at the edge of bubbles around massive stars is explored by JK who confirmed significant dynamical role

of the radiation field in this scenario of massive star formation. In JK and most of the previous numerical simulations of massive star formation, magnetic fields have been neglected for simplicity. We found that magnetic field has a stabilizing role in the radiative RT instability. Although the present study is restricted to the linear perturbations, our results clearly demonstrate that trend of the radiative RT instability is significantly modified when magnetic effects are considered and in order to adequately describe the development of RT instability as a mechanism of creating channels of mass accretion onto young massive stars, this important physical ingredient can not be neglected.

There are also other astrophysical systems where our analysis is applicable. For instance, it has been proposed that clumpy structures in the outflows from supercritical accretion flows are created by the radiative RT instability (e.g., [Takeuchi et al. 2013, 2014](#)). [Takeuchi et al. \(2013\)](#) performed radiation hydrodynamic simulations for a supercritical accretion flows and found that clumps are formed due to RT instability with shapes more or less elongated along the outflow direction. They argued that since formation of clumps are observed in their non-magnetic simulations, mechanisms such as magnetic photon bubble instability is not needed for the clump formation. There are, however, strong theoretical evidences that magnetic fields play a vital role in the accretion flows. If RT instability is responsible for clump formation in these systems, our study shows that magnetic field is able to suppress the instability and not only the clumps may form over a longer period of time but also their size is dependent on the strength of the magnetic field. This issue deserves further investigations.

ACKNOWLEDGMENTS

We are grateful to Mark R. Krumholz for helpful comments and advices. We also thank the anonymous referee for a thoughtful report and constructive suggestions.

REFERENCES

- Basu S., Mouschovias T. C., Paleologou E. V., 1997, [ApJ](#), **480**, L55
- Blaes O., Socrates A., 2003, [ApJ](#), **596**, 509
- Chandrasekhar S., 1961, Hydrodynamic and hydromagnetic stability
- Charbonnel C., Lagarde N., 2010, [A&A](#), **522**, A10
- Díaz A. J., Soler R., Ballester J. L., 2012, [ApJ](#), **754**, 41
- Díaz A. J., Khomeenko E., Collados M., 2014, [A&A](#), **564**, A97
- Hanasz M., Lesch H., 2003, [A&A](#), **412**, 331
- Jacquet E., Krumholz M. R., 2011, [ApJ](#), **730**, 116
- Jiang Y.-F., Davis S. W., Stone J. M., 2013, [ApJ](#), **763**, 102
- Klassen M., Pudritz R. E., Kuiper R., Peters T., Banerjee R., 2016, [ApJ](#), **823**, 28
- Krolik J. H., 1977, [Physics of Fluids](#), **20**, 364
- Krumholz M. R., Matzner C. D., 2009, [ApJ](#), **703**, 1352
- Krumholz M. R., Thompson T. A., 2012, [ApJ](#), **760**, 155
- Krumholz M. R., Klein R. I., McKee C. F., Offner S. S. R., Cunningham A. J., 2009, [Science](#), **323**, 754
- Kuiper R., Klahr H., Beuther H., Henning T., 2012, [A&A](#), **537**, A122
- Kumar M. S. N., 2013, [A&A](#), **558**, A119
- Lowrie R. B., Morel J. E., Hittinger J. A., 1999, [ApJ](#), **521**, 432
- Mathews W. G., Blumenthal G. R., 1977a, [ApJ](#), **214**, 10
- Mathews W. G., Blumenthal G. R., 1977b, [ApJ](#), **214**, 10
- Matsumoto R., Tajima T., Shibata K., Kaisig M., 1993, [ApJ](#), **414**, 357
- Parker E. N., 1966, [ApJ](#), **145**, 811
- Pizzolato F., Soker N., 2006, [MNRAS](#), **371**, 1835
- Ribeyre X., Tikhonchuk V. T., Bouquet S., 2004, [Physics of Fluids](#), **16**, 4661
- Rodrigues L. F. S., Sarson G. R., Shukurov A., Bushby P. J., Fletcher A., 2016, [ApJ](#), **816**, 2
- Rosen A. L., Krumholz M. R., McKee C. F., Klein R. I., 2016, [MNRAS](#), **463**, 2553
- Sarma A. P., Troland T. H., Crutcher R. M., Roberts D. A., 2002, [ApJ](#), **580**, 928
- Shadmehri M., Yaghoobi A., Khajavi M., 2013, [Astrophysics and Space Science](#), **347**, 151
- Shivamoggi B. K., 2008, preprint, ([arXiv:0805.0581](#))
- Stone J. M., Mihalas D., Norman M. L., 1992, [ApJS](#), **80**, 819
- Takeuchi S., Ohsuga K., Mineshige S., 2013, [PASJ](#), **65**, 88
- Takeuchi S., Ohsuga K., Mineshige S., 2014, [PASJ](#), **66**, 48
- Terradas J., Oliver R., Ballester J. L., 2012, [A&A](#), **541**, A102
- Turner N. J., Quataert E., Yorke H. W., 2007, [ApJ](#), **662**, 1052
- Vlemmings W. H. T., Diamond P. J., van Langevelde H. J., Torres J. M., 2006, [A&A](#), **448**, 597

This paper has been typeset from a $\text{\TeX}/\text{\LaTeX}$ file prepared by the author.